

Prenylated Indole Diketopiperazines from the Marine-Derived Fungus *Aspergillus versicolor*

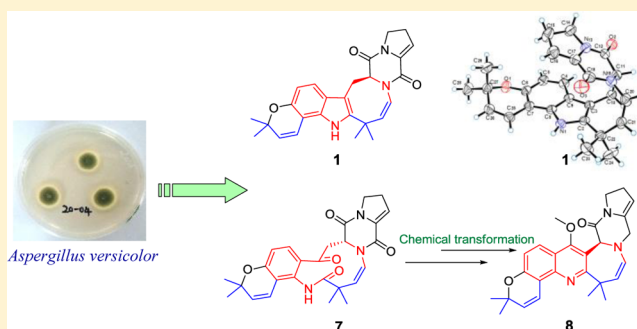
Jixing Peng,[†] Huquan Gao,[†] Jing Li,[†] Jing Ai,[‡] Meiyu Geng,[‡] Guojian Zhang,[†] Tianjiao Zhu,[†] Qianqun Gu,[†] and Dehai Li^{*†}

[†]Key Laboratory of Marine Drugs, Chinese Ministry of Education, School of Medicine and Pharmacy, Ocean University of China, Qingdao 266003, People's Republic of China

[‡]Division of Antitumor Pharmacology, State Key Laboratory of Drug Research, Shanghai Institute of Materia Medica, Chinese Academy of Sciences, Shanghai 201203, People's Republic of China

Supporting Information

ABSTRACT: Seven new prenylated indole diketopiperazines, versicamides A–G (1–7) and a novel chemical derivative from 7, versicamide H (8), along with three known analogic diketopiperazines (9–11) were obtained from the marine-derived fungus *Aspergillus versicolor* HDN08-60. Their structures were determined by spectroscopic techniques, including 2D NMR, ECD calculations, and single-crystal X-ray diffraction analysis, together with the assistance of further chemical conversions. The cytotoxicities of 1–8 were tested against the HeLa, HCT-116, HL-60, and K562 cell lines, but only 8 exhibited moderate activity against HL-60 cells, with an IC₅₀ value of 8.7 μM. Further investigation with target screening showed that 8 exhibited selective PTK inhibitory activities.



INTRODUCTION

Cyclodipeptides with a prenylated indole group, structurally characterized by a diketopiperazine (DKP) ring, bicyclo[2,2,2]-diazaoctane ring, or 1,7-dihydropyrano-[2,3-g]indole ring system, such as brevianamides, paraherquamides, stephacidins, versicolamides, and carneamides, are widely distributed in terrestrial and marine-derived microorganisms, especially in the genera *Penicillium* and *Aspergillus* of Ascomycota.^{1–4} The precursor for this family of natural products is biosynthetically derived from brevianamide F, a modified cyclic dipeptide composed of L-tryptophan and L-proline. Prenylation commonly occurs on N-1, C-2, C-6, C-7, or C-8 of the indole ring.¹ Prenylated indoles containing DKPs have been attractive synthetic targets due to their high structural diversity and wide range of biological activities, including insecticidal, antitumor, anthelmintic, and antibacterial activities.^{1–4} Among the cyclo-(Try-Pro) alkaloids, those containing the 6/5/8/6/5 pentacyclic ring system are rare, with only three cases, including carneamides B and C² along with (+)-deoxyisoaustamide,³ having been reported to our knowledge.

In our ongoing search for prenylated indole derivatives,^{5–14} seven new cyclo-(Try-Pro) alkaloids, versicamides A–G (1–7) and a new derivative versicamide H (8), together with three known ones (9–11)^{15–17} (Supporting Information, Figure S12) were discovered from a marine sediment derived fungus, identified as *Aspergillus versicolor* HDN08-60. Their structures, including the absolute configuration of the known enamide (9),¹⁵ were elucidated on the basis of chemical and

spectroscopic evidence, single-crystal X-ray diffraction analysis, and comparison between the experimental ECD and TDDFT calculated spectra. Compounds 1–6 are characterized by a 6/6/5/8/6/5 hexacyclic ring system containing a hydrogenated azocine moiety, and versicamide G (7) contains a novel 6/6/11/6/5 pentacyclic ring system, whereas versicamide H (8) has an unprecedented skeleton featuring a 2,5-dihydro-1H-azepino-[4,3-*b*]quinoline system. The bioactivity evaluation revealed that versicamide H (8) has moderate cytotoxicity against the HeLa, HCT-116, HL-60, and K562 cell lines (IC₅₀ values: 19.4, 17.7, 8.7, and 22.4 μM, respectively) and inhibitory activity toward various PTKs in vitro, with the highest inhibitory rate of 60% at a concentration of 10 μM in a further target screening program.

RESULTS AND DISCUSSION

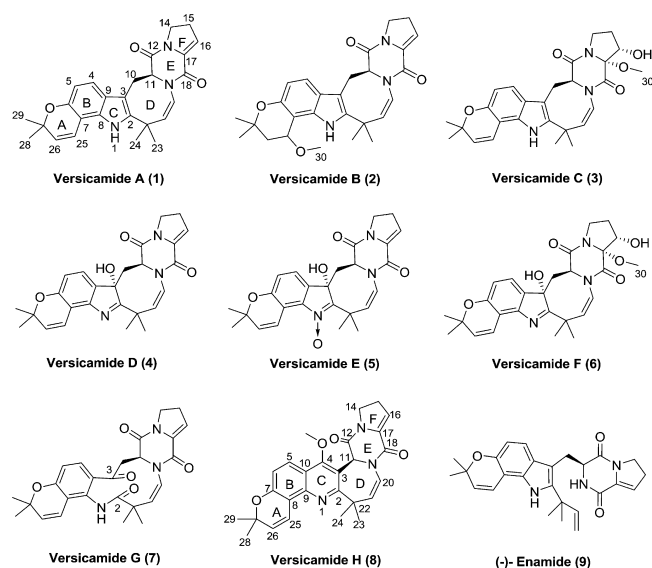
The fungus *Aspergillus versicolor* HDN08-60 was fermented on liquid culture (60 L) for 30 days and extracted three times with EtOAc. The resulting organic extract (12 g) was fractionated by silica gel vacuum liquid chromatography (VLC), Sephadex LH-20 column chromatography, and reversed-phase HPLC to afford seven new compounds (1–7) and three known ones (9–11) (Chart 1).

Versicamide A (1) was obtained as colorless crystals. The molecular formula was determined to be C₂₆H₂₇N₃O₃ on the

Received: May 9, 2014

Published: August 4, 2014

Chart 1



basis of the HRESIMS ion at m/z 430.2127 $[M + H]^+$, indicating 15 degrees of unsaturation. The 1D NMR data (Table 1) suggested the presence of 26 carbon resonances,

including 4 methyls, 3 methylenes with geminal nonequivalent protons, an aliphatic methine, 7 olefinic methines, and 11 carbons without hydrogens attached including 2 amides.

The tetrasubstituted indole moiety in **1** was deduced by the HMBC correlations from H-4 to C-3, C-6, and C-8; from H-5 to C-6, C-7, and C-9; and from NH-1 to C-2, C-3, C-8, and C-9, together with the ^1H - ^1H COSY correlation between H-4 and H-5 (Figure 1). The diketopiperazine ring was suggested by the characteristic NMR data of CH-11 (δ_{H} 4.32, δ_{C} 59.2), C-12 (δ_{C} 161.6), and C-18 (δ_{C} 155.0).^{2,3} The unsaturated proline moiety was indicated by the ^1H - ^1H COSY correlations of H-14/H-15/H-16 and by the HMBC correlations from H-15/H-16 to C-17. The indole and diketopiperazine rings were cyclized and formed an azocane ring, which was supported by the COSY correlations (H-10/H-11, H-20/H-21) and HMBC correlations from H-10 to C-2, C-3, C-9, and C-12; from H-20 to C-18 and C-22; from H-21 to C-2 and C-23; and from H-24 to C-2, C-22, and C-23. Finally, the core structure was established by the attachment of an oxygenated isoprenyl group to C-6 and C-7, which was supported by the molecular formula and the HMBC correlations from H-25 to C-6, C-7, C-8, and C-27; from H-28/29 to C-26 and C-27, along with the COSY correlations between H-25 and H-26, in addition to the chemical shifts of C-6 (δ_{C} 147.0) and C-27 (δ_{C} 74.6). The structure of **1** was further confirmed by X-ray crystallographic

Table 1. ^1H and ^{13}C NMR Data for Compounds 1–3 in $\text{DMSO}-d_6$

no.	1 ^a		2 ^b		3 ^b	
	δ_{C} , mult	δ_{H} (J in Hz)	δ_{C} , mult	δ_{H} (J in Hz)	δ_{C} , mult	δ_{H} (J in Hz)
1-NH		10.14 (s)		9.28 (s)		10.22 (s)
2	140.2, C		139.2, C		139.8, C	
3	102.6, C		102.4, C		103.3, C	
4	117.0, CH	6.98 (d, 8.5)	118.1, CH	7.05 (d, 8.5)	117.5, CH	7.03 (d, 8.5)
5	108.8, CH	6.44 (d, 8.5)	109.5, CH	6.40 (d, 8.5)	109.3, CH	6.42 (d, 8.5)
6	147.0, C		148.6, C		147.3, C	
7	104.3, C		104.0, C		104.4, C	
8	130.9, C		133.5, C		131.2, C	
9	122.9, C		121.8, C		123.4, C	
10	26.0, CH ₂	3.22 (dd, 14.8, 6.6); 3.32 (d, 14.8)	26.1, CH ₂	3.21 (dd, 15.0, 6.5); 3.33 (d, 15.0)	26.0, CH ₂	3.18 (dd, 15.0, 6.7); 3.48 (d, 14.9)
11	59.2, CH	4.32 (d, 6.6)	59.4, CH	4.32 (d, 6.5)	58.4, CH	4.16 (d, 6.7)
12	161.6, C		161.8, C		166.3, C	
14	44.9, CH ₂	3.42 (m); 3.65 (m)	45.2, CH ₂	3.40 (m); 3.65 (m)	42.7, CH ₂	2.71 (m); 3.94 (m)
15	26.6, CH ₂	1.99 (m); 2.34 (m)	26.8, CH ₂	2.02 (m); 2.32 (m)	28.8, CH ₂	1.51 (m); 1.83 (m)
16	117.0, CH	5.48 (t, 2.8)	117.4, CH	5.50 (t, 2.8)	74.2, CH	3.90 (m)
16-OH						5.43 (d, 4.9)
17	132.0, C		132.1, C		93.9, C	
18	155.0, C		155.3, C		162.0, C	
20	121.1, CH	5.72 (d, 8.8)	121.5, CH	5.73 (d, 8.8)	121.7, CH	5.76 (d, 8.8)
21	141.1, CH	5.76 (d, 8.8)	141.2, CH	5.77 (d, 8.8)	140.9, CH	5.79 (d, 8.8)
22	37.2, C		37.1, C		37.3, C	
23	31.8, CH ₃	1.31 (s)	31.8, CH ₃	1.32 (s)	32.2, CH ₃	1.33 (s)
24	26.2, CH ₃	1.54 (s)	26.0, CH ₃	1.51 (s)	28.4, CH ₃	1.54 (s)
25	118.5, CH	7.08 (d, 9.9)	68.9, CH	4.89 (t, 6.0)	118.4, CH	6.98 (d, 9.8)
26	128.2, CH	5.68 (d, 9.9)	35.9, CH ₂	2.02 (dd, 2.7, 6.0)	128.6, CH	5.64 (d, 9.8)
27	74.6, C		74.1, C		74.9, C	
28	26.8, CH ₃	1.33 (s)	27.5, CH ₃	1.35 (s)	27.0, CH ₃	1.31 (s)
29	26.5, CH ₃	1.36 (s)	26.5, CH ₃	1.24 (s)	27.0, CH ₃	1.32 (s)
30			53.4, CH ₃	3.30 (s)	47.5, CH ₃	1.56 (s)

^aSpectra were recorded at 600 MHz for ^1H NMR and at 150 MHz for ^{13}C NMR using $\text{DMSO}-d_6$ as solvent. ^bSpectra were recorded at 400 MHz for ^1H NMR and at 100 MHz for ^{13}C NMR using $\text{DMSO}-d_6$ as solvent.

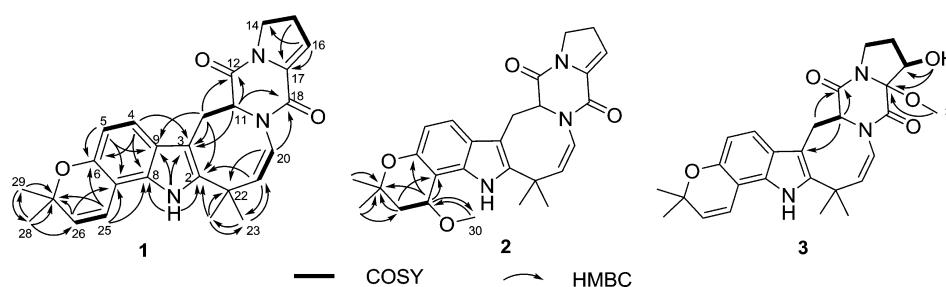


Figure 1. Key ^1H - ^1H COSY and HMBC correlations of 1–3.

analysis (Supporting Information, Figure S1), which revealed the *S* absolute configuration at C-11. Compound 1 was stable when stirred in CHCl_3 -MeOH with the presence of silica gel and in CHCl_3 -MeOH- H_2O under acidic conditions (pH 5) for 24 h.

The molecular formula of versicamide B (2) was determined to be $\text{C}_{27}\text{H}_{31}\text{N}_3\text{O}_4$ based on the HRESIMS ion at m/z 462.2385 $[\text{M} + \text{H}]^+$, which differed from 1 by 32 amu. The 1D NMR data (Table 1) of 2 were similar to those of 1, the only difference was that the double bond Δ^{25} in 1 was replaced by the methoxylated single bond in 2. The structural difference was assigned by ^1H - ^1H COSY correlation between H-25 (δ_{H} 4.89) and H-26 (δ_{H} 2.02) as well as key HMBC correlations from H-25 to C-6 (δ_{C} 148.6), C-7 (δ_{C} 104.0), C-27 (δ_{C} 74.1), and C-30 (δ_{C} 53.4); from H-26 to C-7 and C-27; and from H-30 (δ_{H} 3.30, *s*) to C-25 (δ_{C} 68.9) (Figure 1). The absolute configuration of C-11 in 2 was proposed to be the same as that of 1 based on their almost identical chemical shifts as well as a consideration of their biogenetic relationship (Scheme 2), although the stereochemistry for C-25 could not be determined by the ECD calculation or other methods as a result of the instability of 2.

Versicamide C (3) was assigned a molecular formula of $\text{C}_{27}\text{H}_{31}\text{N}_3\text{O}_5$ by the HRESIMS ion at 478.2339 $[\text{M} + \text{H}]^+$. A direct comparison of the ^1H and ^{13}C NMR data (Table 1) with those of 1 revealed that they share the similar structure, except that 3 has a oxidized proline moiety, which was further confirmed by the COSY correlations H-14/H-15/H-16/16-OH and HMBC correlations of 16-OH/C-16 (δ_{C} 74.2), C-17 (δ_{C} 93.9), and of H-30/C-17 (Figure 1).

The relative configuration of 3 was deduced to be 11*S**,16*S**,17*R** based on the NOEs from H-16 to H-24 (4.351 Å) and from H-11 to H-30 (3.412 Å) (Figure 2). The absolute configuration of 3 could be proposed on the basis of biogenetic considerations (Scheme 2) and was unambiguously determined as 11*S*,16*S*,17*R* based on the ECD calculation (Figure 3).

Versicamide D (4) was obtained as a white amorphous solid, and its molecular formula was determined to be $\text{C}_{26}\text{H}_{27}\text{N}_3\text{O}_4$ based on HRESIMS, revealing a 16 amu increase in the molecular weight compared with that of 1. In comparison to 1, compound 4 has a hydroxy group attached to C-3, which was supported by the HMBC correlations from 3-OH (δ_{H} 5.67) to C-2 (δ_{C} 188.80) and C-3 (δ_{C} 84.71). The gross structure was further confirmed by analysis of the 1D and 2D NMR data (Table 2 and Figure 4). Arising from the two chiral centers at C-3 and C-11, four possible diastereomers exist belonging to two pairs of relative configurations, 3*S**,11*S** and 3*R**,11*S**. The absolute configuration of 4 was finally established by the comparison of the ECD experimental data with the theoretical spectrum. Density functional theory (DFT) calculations

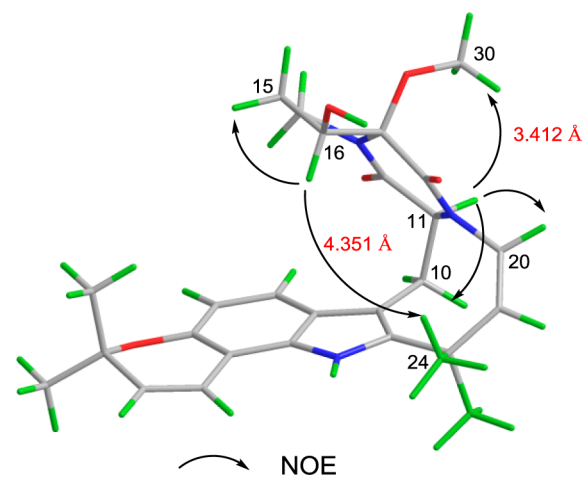


Figure 2. Key NOE correlations of 3 and corresponding interatomic distances.

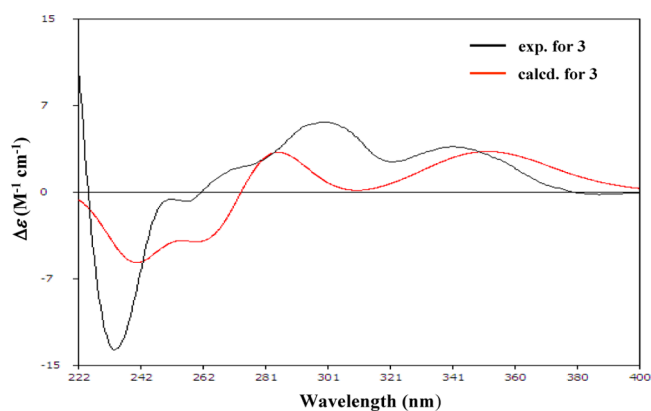


Figure 3. B3LYP/6-31+g(d)-calculated ECD spectrum of (11*S*,16*S*,17*R*)-3 (red) and the experimental ECD spectrum of 3 (black) ($\sigma = 0.26$ eV).

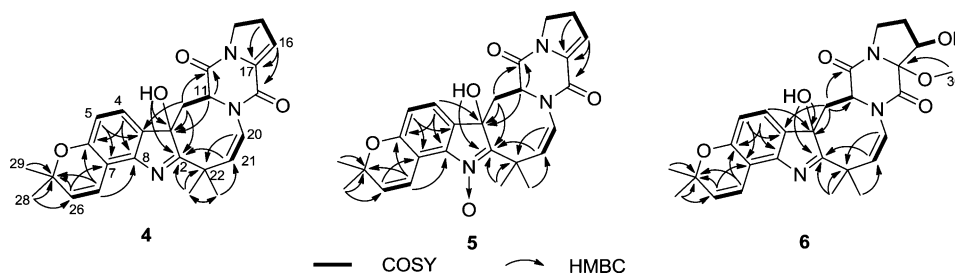
performed at the B3LYP/6-311+G** level were used to generate ECD spectra for the respective lowest-energy conformers of (3*S*,11*S*)-4 and (3*R*,11*S*)-4, suggesting 3*S*,11*S* absolute configuration of 4 (Figure 5).

The molecular formula of versicamide E (5) was determined to be $\text{C}_{26}\text{H}_{27}\text{N}_3\text{O}_5$ based on the HRESIMS $[\text{M} + \text{H}]^+$ ion at m/z 462.2024, exhibiting 16 amu more than that of 4. The HRESIMS spectrum displayed a significant fragment peak at m/z 446.2079 $[\text{M} - 16 + \text{H}]^+$, suggesting the presence of an N-oxide function. The structure of 5 was finally established as the N-1 oxide of 4 based on intensive analysis of both 1D and 2D NMR spectra (Table 2 and Figure 4), the consideration of similar structures in the literatures,^{1,4} and the chemical

Table 2. ^1H and ^{13}C NMR Data for Compounds 4–6 in $\text{DMSO-}d_6$ and for Compound 7 in CDCl_3

no.	4^a		5^b		6^a		7^c	
	δ_{C} , mult	δ_{H} (J in Hz)	δ_{C} , mult	δ_{H} (J in Hz)	δ_{C} , mult	δ_{H} (J in Hz)	δ_{C} , mult	δ_{H} (J in Hz)
1-NH								7.75
2	188.80, C		188.78, C		189.1, C		176.1, C	
3	84.71, C		84.71, C		84.3, C		202.4, C	
3-OH		5.67 (s)		5.69 (s)		5.67 (s)		
4	124.11, CH	6.87 (d, 7.9)	124.11, CH	6.86 (d, 7.9)	125.0, CH	6.89 (d, 8.0)	129.4, CH	7.27 (overlapped)
5	112.55, CH	6.50 (d, 7.9)	112.54, CH	6.50 (d, 7.9)	111.8, CH	6.49 (d, 8.0)	116.7, CH	6.82 (d, 8.5)
6	153.97, C		153.98, C		153.3, C		157.3, C	
7	113.72, C		113.72, C		112.4, C		117.2, C	
8	148.92, C		148.94, C		148.2, C		no signal	
9	131.94, C		131.93, C		131.6, C		128.2, C	
10	38.83, CH_2	2.78 (dd, 14.2, 6.7); 2.84 (d, 14.2)	38.83, CH_2	2.78 (dd, 14.2, 6.7); 2.85 (d, 14.2)	37.9, CH_2	2.74 (dd, 14.3, 6.6); 2.99 (d, 14.3)	43.6, CH_2	3.27 (br s); 3.75 (br s)
11	58.57, CH	4.04 (d, 6.7)	58.59, CH	4.04 (d, 6.7)	56.6, CH	4.26 (d, 6.3)	59.3, CH	4.44 (br s)
12	160.67, C		160.68, C		163.9, C		163.5, C	
14	45.55, CH_2	3.16 (m); 3.42 (m)	45.54, CH_2	3.16 (m); 3.41 (m)	39.5, CH_2	2.51 (m); 2.89 (m)	46.5, CH_2	4.08 (m); 4.28 (m)
15	27.28, CH_2	2.19 (m); 2.38 (m)	27.28, CH_2	2.17 (m); 2.39 (m)	26.8, CH_2	1.47 (m); 1.64 (m)	28.6, CH_2	2.90 (m); 3.02 (m)
16	117.37, CH	5.65 (t, 2.8)	117.34, CH	5.65 (t, 2.8)	73.4, CH	3.42 (m)	127.1, CH	6.53 (t, 3.1)
16-OH						4.73 (d, 7.2)		
17	132.62, C		132.64, C		86.4, C		130.8, C	
18	154.53, C		154.54, C		163.3, C		157.3, C	
20	121.30, CH	5.59 (d, 7.9)	121.30, CH	5.58 (d, 7.9)	121.4, CH	5.75 (d, 7.9)	124.1, CH	5.70 (br s)
21	141.95, CH	5.82 (d, 7.9)	141.95, CH	5.82 (d, 7.9)	140.6, CH	5.89 (d, 7.9)	138.8, CH	5.86 (d, 9.2)
22	41.97, C		41.96, C		41.3, C		43.1, C	
23	27.58, CH_3	1.46 (s)	27.58, CH_3	1.45 (s)	26.4, CH_3	1.47 (s)	27.5, CH_3	1.65 (br s)
24	26.25, CH_3	1.36 (s)	26.24, CH_3	1.35 (s)	28.2, CH_3	1.38 (s)	27.5, CH_3	1.52 (br s)
25	117.92, CH	6.70 (d, 9.8)	117.90, CH	6.70 (d, 9.8)	116.7, CH	6.78 (d, 10.0)	115.1, CH	6.19 (d, 10.1)
26	131.34, CH	5.77 (d, 9.8)	131.33, CH	5.77 (d, 9.8)	131.4, CH	5.84 (d, 10.0)	133.7, CH	5.80 (d, 10.1)
27	76.51, C		76.52, C		76.2, C		77.4, C^d	
28	28.90, CH_3	1.42 (s)	28.89, CH_3	1.41 (s)	28.4, CH_3	1.45 (s)	28.1, CH_3	1.48 (s)
29	28.18, CH_3	1.30 (s)	28.16, CH_3	1.30 (s)	27.5, CH_3	1.34 (s)	28.1, CH_3	1.38 (s)
30					49.8	2.90 (s)		

^aSpectra were recorded at 400 MHz for ^1H NMR and at 100 MHz for ^{13}C NMR using $\text{DMSO-}d_6$ as solvent. ^bSpectra were recorded at 500 MHz for ^1H NMR and at 125 MHz for ^{13}C NMR using $\text{DMSO-}d_6$ as solvent. ^cSpectra were recorded at 400 MHz for ^1H NMR and at 100 MHz for ^{13}C NMR using CDCl_3 (adding TFA) as solvent. ^dSignal overlapped.

Figure 4. Key ^1H – ^1H COSY and HMBC correlations of 4–6.

characteristics of amide (N-13 and N-19) and imine (N-1). The absolute configuration of **5** was further determined as 3*S*,11*S* by comparing the ECD spectrum of **5** with that of **4** (Figure 6).

Versicamide F (**6**) was assigned the molecular formula $\text{C}_{27}\text{H}_{31}\text{N}_3\text{O}_6$ by the HRESIMS ion at 494.2293 $[\text{M} + \text{H}]^+$. A direct comparison of the ^1H and ^{13}C NMR data (Table 2) with those of **3** and **4** revealed the core structure as shown in Figure 4, which was further confirmed by the 2D NMR correlations (Figure 4). The relative configuration of **6** was deduced to be 3*S**,11*S**,16*S**,17*R** based on its similar chemical shifts in

comparison with those of compounds **3** and **4** together with the NOESY correlations of H-16 with H-25 (4.746 Å), H-11 with H-30 (3.942 Å), and of 3-OH with H-24 (2.909 Å) (Figure 7). The absolute configuration of **6** was further determined to be 3*S*,11*S*,16*S*,17*R* by comparing its ECD spectrum (Figure 6) with that of compound **4** as well as based on biogenetic considerations (Scheme 1).

The molecular formula of versicamide G (**7**) was determined to be $\text{C}_{26}\text{H}_{27}\text{N}_3\text{O}_5$ based on a HRESIMS $[\text{M} + \text{H}]^+$ ion at m/z 462.2024 (calcd. 462.2023). **7** in CD_3CN and in $\text{DMSO-}d_6$

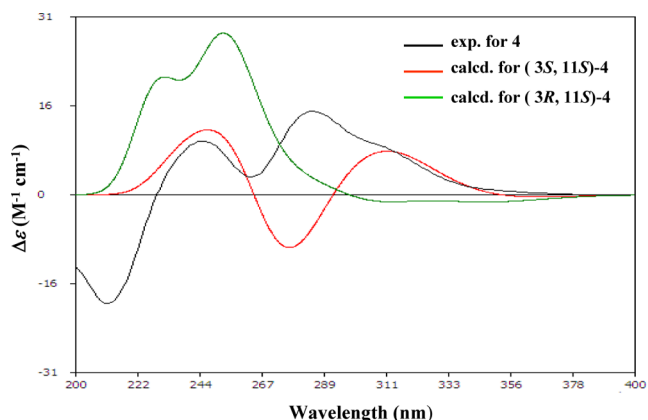


Figure 5. B3LYP/6-311+g(d,p)-calculated ECD spectra of (3S,11S)-4 (red) and (3R,11S)-4 (green) and experimental ECD spectrum of 4 (black) ($\sigma = 0.30$ eV).

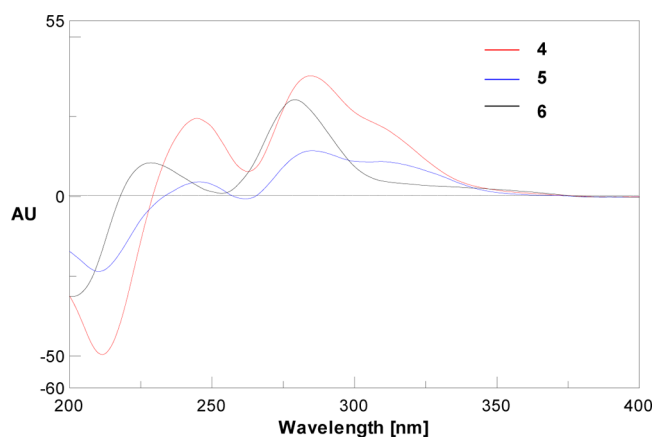


Figure 6. Experimental ECD spectra of compounds 4–6.

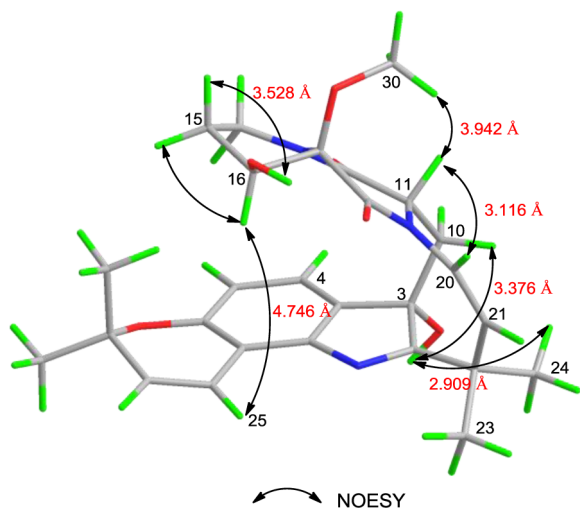


Figure 7. Key NOESY correlations of 6 and corresponding interatomic distances.

only exhibited partial NMR data (Supporting Information, Figure S62–S65), which was sufficient to elucidate only a partial structure of 7 and suggested that 7 was one of the homologues of compounds 1–6. A chemical modification experiment was sufficient to elucidate the complete structure of 7. Considering the methylation derivative 8 (vide infra), the

structure of 7 was proposed and further confirmed by the NMR data obtained in CDCl_3 with a drop of TFA (Table 2). The ^{13}C NMR data showed the presence of lactam ($\delta_{\text{C}} 176.1$, C-2) and ketone ($\delta_{\text{C}} 202.4$, C-3) carbonyls. The linkage of C-2 to C-22 was supported by the HMBC correlations from H_3 -24 to C-2, C-22, and C-21 (Figure 8). Unfortunately, direct evidence to

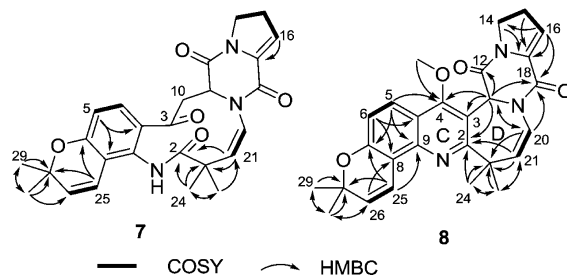


Figure 8. Key ^1H – ^1H COSY and HMBC correlations of 7 and 8.

establish the structure was lacking due to the absence of the 1D NMR signal for C-8 and HMBC signals correlated to H_2 -10. In order to further confirm the proposed structure, a chemical conversion starting from compound 4 (Scheme 1) was carried out. Structurally, we supposed that compound 7 would be generated from 4 through acid-catalyzed oxidation.¹⁸ Indeed, compound 4 was treated with TFA in DMSO (H_2O) for 10 days at room temperature, which afforded compound 7. The cyclic lactam in 7 could be formed by a hydrolyzation of imine with acid, accompanied by cleavage of the intermediate glycol (Scheme 1). Thus, the structure of 7 was confirmed. The absolute configuration of 7 was further determined as 11S based on biogenetic considerations and ECD calculations (Figure 9). Compound 7 possesses a rare type of skeleton, featuring a (*Z*)-7,8-dihydro-1*H*-benzo[*g*][1,6]-diazacycloundecine-2,9(3*H*,6*H*)-dione moiety.

An unexpected product, versicamide H (8), was obtained from the methylation reaction of 7. The molecular formula of $\text{C}_{27}\text{H}_{27}\text{N}_3\text{O}_4$ was established based on HRESIMS (m/z 458.2075, calcd. for $\text{C}_{27}\text{H}_{28}\text{N}_3\text{O}_4$ 458.2074) and ^{13}C NMR data (Table 3), indicating 16 degrees of unsaturation. Careful analysis of 1D NMR (Table 3) spectra revealed the presence of 2 amide/carbonyl carbons (C-12 and C-18), 9 sp^2 carbons without hydrogen attached, 7 olefinic methines, 1 aliphatic methine, 2 methylenes with geminal nonequivalent protons, and 5 methyls (1 oxygenated), indicating that 6 rings were required to satisfy the 16 degrees of unsaturation.

The 1D NMR data indicated that 8 contained the same motifs of rings A, B, E, and F as those in 1. Ring D was established by the ^1H – ^1H COSY correlations between H-20 and H-21 and by the HMBC correlations from H_3 -23/ H_3 -24 to C-2, C-21, and C-22; from H-11 to C-2, C-3, C-12, C-18, and C-20; and from H-20 to C-11, C-18, and C-22. Finally, the core structure was determined by the establishment of the ring C based on key HMBC correlations from H-5 to C-4 and C-9, from H-6 to C-10, and from H-25 to C-9, the molecular formula, and the attachment of the methoxy group to C-4 according to the HMBC correlation (Figure 8).

The *Z,Z* configurations of the two double bonds in the isoprenyl units were determined from the coupling constants ($^3J_{\text{H-20, H-21}} = 10.4$ Hz, $^3J_{\text{H-25, H-26}} = 10.0$ Hz) (Table 3). The chemical transformation from 7 to 8, possibly through a base-catalyzed internal condensation¹⁹ (7 to 7a) and intramolecular enol–keto interconversion (7a to 7b) (Scheme 1), allowed us

Scheme 1. Chemical Transformation and Possible Mechanism from 4 to 7 and from 7 to 8

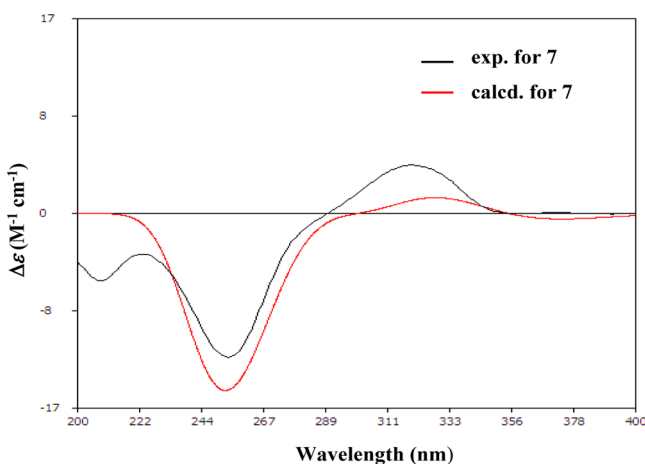
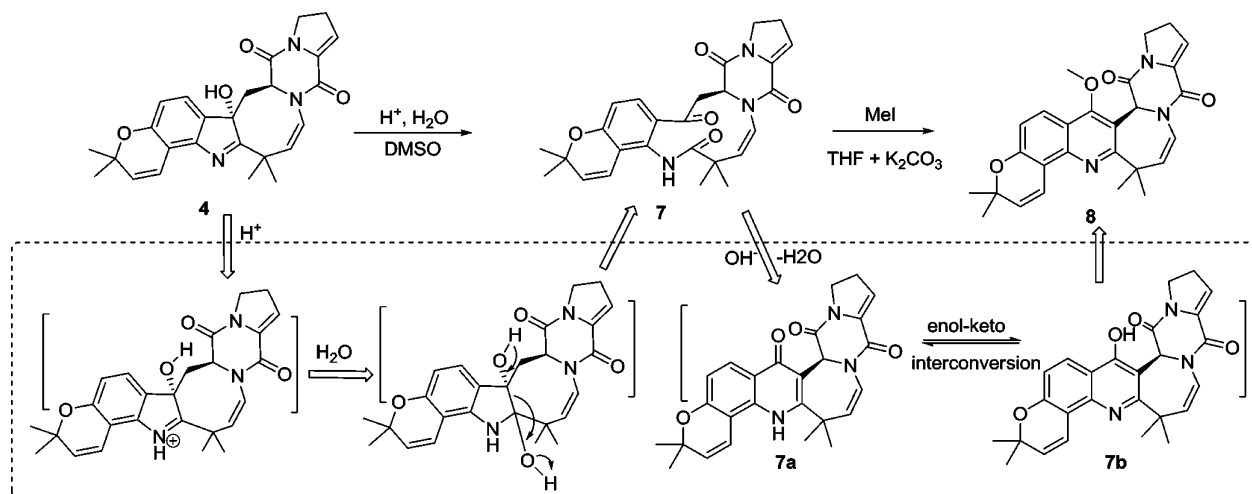


Figure 9. B3LYP/6-311+g(d,p)-calculated ECD spectrum of (11S)-7 (red) and experimental ECD spectrum of 7 (black) ($\sigma = 0.36$ eV).

to establish the 11S absolute configuration of the novel unnatural compound 8, which was consistent with that of ECD calculations (Figure 10).

The biosynthesis of the isolated indole alkaloids was proposed as shown in Scheme 2. Compound 1 may be biogenetically derived from (–)-enamide (9) via cyclization between the diketopiperazine moiety and the isoprenyl unit, and compounds 2–7 were proposed to be derived from 1 followed by further oxidation and methylation.

New compounds 1–8 were evaluated for their cytotoxic activity against the HeLa and HCT-116 cancer cell lines using the MTT method^{20,21} as well as against the HL-60 and K562 cell lines using the SRB method.^{20,22} Only compound 8 exhibited moderate cytotoxicities, with IC_{50} values of 19.4, 17.7, 8.7, and 22.4 μ M, respectively, whereas compounds 1–7 were virtually inactive with $IC_{50} > 50$ μ M. In addition, compound 8 was further tested for its inhibitory activity toward 18 selected PTKs in vitro using enzyme-linked immunosorbent assay (ELISA).²³ As shown in Table 4, compound 8 showed effective activity on c-Kit as one of the PTKs tested, yielding an inhibitory rate of 60% at a final concentration of 10 μ M. Meanwhile, compound 8 showed slight inhibitory effects on KDR, RET, and EGFR kinases, with inhibitory rates ranging from 23 to 35% at a concentration of 10 μ M. Toward the

remained PTKs assay, however, compound 8 failed to exhibit inhibitory activity.

In summary, a chemistry study of a marine-derived fungal strain led to the isolation of eight new isoprenylated indole alkaloids. Single-crystal X-ray diffraction, ECD calculations, and chemical derivatization methods were employed to determine the absolute configuration. Inspiringly, the skeletons of versicamide G (7) and versicamide H (8) possess unprecedented ring systems. Versicamide H (8) showed cytotoxicity and inhibited the activity of various PTKs in vitro.

EXPERIMENTAL SECTION

General Experimental Procedures. Optical rotations were measured in MeOH using a 10 cm microcell. UV spectra were recorded from 200 to 600 nm on a spectrophotometer. ECD spectra were measured in MeOH from 200 to 400 nm on a spectropolarimeter. IR spectra were recorded on a spectrophotometer in KBr discs. NMR spectra were recorded on 400, 500, and 600 MHz spectrometers using TMS as an internal standard. The 1D and 2D NMR spectra were performed using standard software. HRESIMS spectra were performed on a Q-TOF mass spectrometer. X-ray crystal data were measured with Cu $K\alpha$ radiation at 293 K. Semipreparative HPLC was performed using an ODS column (5 μ m, 10 \times 250 mm, 4 mL/min). TLC and column chromatography (CC) were performed on plates precoated with silica gel GF254 (10–40 μ m) or over silica gel (200–300 mesh). Size-exclusion chromatography was performed using Sephadex LH-20.

Fungal Material. The fungal strain *Aspergillus versicolor* HDN08-60 was isolated from the sediments (depth, 35 m) collected in the South China Sea (22°10'N, 114°38'E) and was identified by ITS sequence. A voucher specimen is deposited in our laboratory at –20 °C. The working strain was prepared on potato dextrose agar slants and stored at 4 °C.

Fermentation and Extraction. The fungus HDN08-60 was cultured under static conditions at 28 °C in 1 L Erlenmeyer flasks containing 300 mL of liquid culture medium composed of maltose (10.0 g/L), mannitol (20.0 g/L), glucose (20.0 g/L), peptone (5.0 g/L), yeast extract (3.0 g/L), potato (200.0 g/L), and seawater (Huiquan Bay, Yellow Sea). After 30 days of cultivation, 60 L of whole broth was filtered through cheese cloth to separate the supernatant from the mycelia. The former was extracted three times with EtOAc, and the latter was extracted three times with acetone and concentrated under reduced pressure to afford an aqueous solution that was extracted three times with EtOAc. The EtOAc solutions were combined and concentrated under reduced pressure to give total organic extract (12 g).

Purification. The organic extract was subjected to vacuum liquid chromatography over silica gel column using a gradient elution with

Table 3. One-Dimensional^a and Two-Dimensional NMR Data for Compound 8 in DMSO-*d*₆

no.	δ_C , mult	δ_H (J in Hz)	¹ H- ¹ H COSY	HMBC (¹ H → ¹³ C)
2	165.3, C			
3	118.4, C			
4	161.2, C			
4-OCHH ₃	63.7	3.85 (s)		4
5	122.9, CH	7.80 (d, 9.1)	6	4, 7, 9
6	118.2, CH	7.10 (d, 9.1)	5	8, 10
7	153.7, C			
8	115.5, C			
9	144.0, C			
10	116.1, C			
11	57.4, CH	6.04 (s)		2, 3, 4, 12, 18, 20
12	159.9, C			
14	45.5, CH ₂	3.99 (m); 4.17 (m)	15	17
15	27.9, CH ₂	2.80 (m); 2.91 (m)	14, 16	17
16	120.6, CH	6.25 (t, 3.2)	15	14, 17, 18
17	132.6, C			
18	152.7, C			
20	123.0, CH	6.81 (d, 10.4)	21	11, 18, 22
21	121.2, CH	5.06 (d, 10.4)	20	2, 22, 23, 24
22	43.0, C			
23	32.5, CH ₃	1.70 (s)		2, 21, 22, 24
24	32.1, CH ₃	1.67 (s)		2, 22, 21, 23
25	117.4, CH	7.35 (d, 10.0)	26	7, 9, 27
26	129.6, CH	5.83 (d, 10.0)	25	8, 28
27	77.1, C			
28	27.8, CH ₃	1.45 (s)		26, 27, 29
29	27.5, CH ₃	1.43 (s)		28, 27

^aFor 1D NMR, 400 MHz for ¹H and 100 MHz for ¹³C.

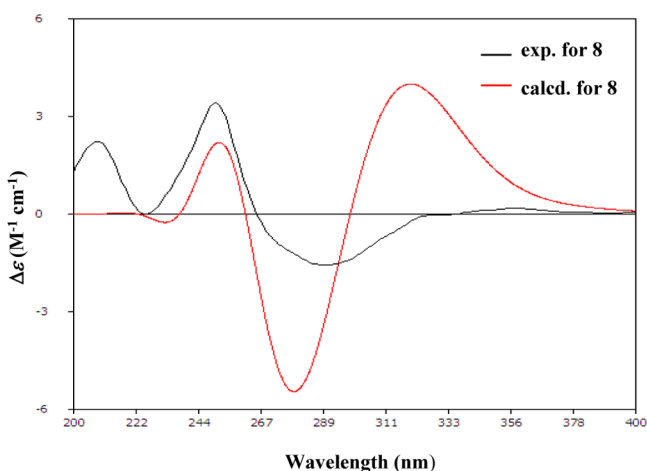


Figure 10. B3LYP/6-31+g(d)-calculated ECD spectrum of (11S)-8 (red) and experimental ECD spectrum of 8 (black) ($\sigma = 0.33$ eV).

CHCl₃-MeOH to give three fractions [fraction 1 (CHCl₃-MeOH; 500:1 to 200:1), fraction 2 (CHCl₃-MeOH; 200:1 to 100:1), and fraction 3 (CHCl₃-MeOH; 100:1 to 50:1)]. Fraction 1 was separated by Sephadex LH-20, eluting with CHCl₃-MeOH (1:1) to provide two subfractions (fraction 1.1 and fraction 1.2). Fraction 1.1 was purified by semipreparative HPLC (55:45 MeOH-H₂O, 4 mL/min) to afford compound 1 (100 mg). Fraction 1.2 was further separated by semipreparative HPLC (60:40 MeOH-H₂O, 4 mL/min) to give compound 11 (50 mg). Fraction 2 was rechromatographed on Sephadex LH-20 to provide three fractions (fractions 2.1-2.3). Fractions 2.1 and 2.2 were further purified by MPLC to give fractions 2.1.1 and 2.2.1, respectively. Fraction 2.1.1 was purified by semipreparative HPLC (45:50 MeOH-H₂O, 4 mL/min) to give

compounds 4 (40 mg) and 5 (11 mg). Fractions 2.2.1 and 2.3 were further purified by semipreparative HPLC (55:50 MeOH-H₂O, 4 mL/min) to give compounds 9 (68 mg; from fraction 2.2.1), 10 (27 mg; from fraction 2.2.1), and 2 (6 mg; from fraction 2.2.2), respectively. Fraction 3 was purified by Sephadex LH-20, eluting with MeOH, and then on a semipreparative HPLC column (55:35 MeOH-H₂O, 4 mL/min) to afford compounds 3 (9 mg), 6 (4 mg), and 7 (35 mg).

Versicamide A (1). Colorless crystal; mp 240 °C; $[\alpha]_D^{25} +123$ (c 0.1, CHCl₃); UV (MeOH) λ_{\max} (log ϵ) 257 (4.5), 287 (3.9), 296 (3.7), 325 (3.6); ECD (0.69×10^{-3} M, MeOH) λ_{\max} ($\Delta\epsilon$) 338 (+2.71), 306.5 (-2.48), 274 (9.13), 241.5 (-8.78), 227.5 (+2.26), 213.5 (-8.85) nm; IR (KBr) ν_{\max} 3347, 1675, 1643, 1446, 1374, 1156, 1119 cm⁻¹; ¹H and ¹³C NMR data (see Table 1); HRESIMS $[M + H]^+ m/z$ 430.2127 (calcd. for C₂₆H₂₈N₃O₃, 430.2125).

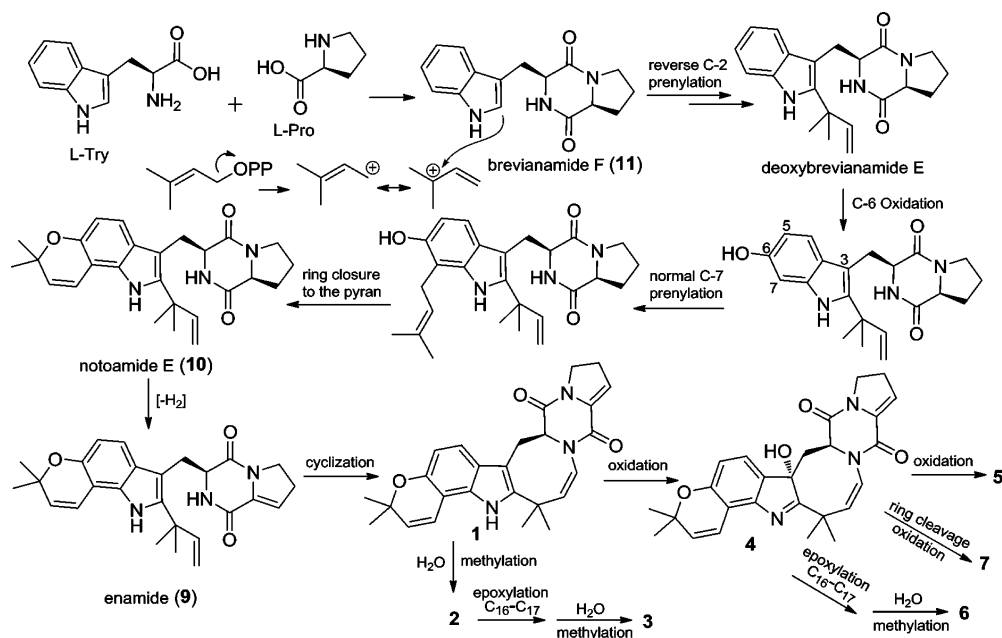
Versicamide B (2). White amorphous solid; ¹H and ¹³C NMR (see Table 1); HRESIMS $[M + H]^+ m/z$ 462.2385 (calcd. for C₂₇H₃₂N₃O₄, 462.2387).

Versicamide C (3). White amorphous solid; $[\alpha]_D^{25} +274$ (c 0.1, CHCl₃); UV (MeOH) λ_{\max} (log ϵ) 259 (4.5), 287 (3.9), 296 (3.7), 325 (3.6); ECD (1.04×10^{-3} M, MeOH) λ_{\max} ($\Delta\epsilon$) 340.5 (+2.42), 320.5 (+1.47), 302 (+3.24), 233.5 (-8.56) nm; IR (KBr) ν_{\max} 3345, 1676, 1643, 1447, 1374 cm⁻¹; ¹H and ¹³C NMR (see Table 1); HRESIMS $[M + H]^+ m/z$ 478.2339 (calcd. for C₂₇H₃₂N₃O₅, 478.2336).

Versicamide D (4). White amorphous solid; $[\alpha]_D^{25} +170$ (c 0.07, CHCl₃); UV (MeOH) λ_{\max} (log ϵ) 265 (4.5), 287 (3.9), 296 (3.7), 325 (3.6); ECD (1.12×10^{-3} M, MeOH) λ_{\max} ($\Delta\epsilon$) 350 (+0.52), 315 (+5.07), 302 (+6.73), 284.5 (+13.81), 262.5 (+2.99) 245 (+8.89), 211.5 (-18.17) nm; IR (KBr) ν_{\max} 3400, 1744, 1676, 1644, 1445, 1377, 1162 cm⁻¹; ¹H and ¹³C NMR (see Table 2); HRESIMS $[M + H]^+ m/z$ 446.2075 (calcd. for C₂₆H₂₇N₃O₄, 446.2074).

Versicamide E (5). White amorphous solid; $[\alpha]_D^{25} +124$ (c 0.04, CHCl₃); UV (MeOH) λ_{\max} (log ϵ) 265 (4.5), 287 (3.9), 296 (3.7), 325 (3.6); ECD (0.65×10^{-3} M, MeOH) λ_{\max} ($\Delta\epsilon$) 350 (+0.58), 318

Scheme 2. Plausible Biosynthetic Pathways of 1–7 and 9–11



(+4.57), 301 (+5.09), 285 (+6.69), 261.5 (−0.35), 245.5 (+2.14), 210 (−10.98) nm; IR (KBr) ν_{\max} 3400, 1744, 1676, 1644, 1445, 1377, 1162 cm^{-1} ; ^1H and ^{13}C NMR (see Table 2); HRESIMS $[\text{M} + \text{H}]^+ m/z$ 462.2024 (calcd. for $\text{C}_{26}\text{H}_{28}\text{N}_3\text{O}_5$, 462.2023).

Versicamide F (6). White amorphous solid; $[\alpha]_{\text{D}}^{25} +21$ (c 0.06, CHCl_3); UV (MeOH) λ_{\max} (log ϵ) 268 (4.5), 287 (3.9), 296 (3.7), 325 (3.6); ECD (1.01×10^{-3} M, MeOH) λ_{\max} ($\Delta\epsilon$) 349 (+0.67), 306 (+1.81), 279 (+9.08), 253.5 (+0.29), 228.5 (+3.15), 205 (−8.82) nm; IR (KBr) ν_{\max} 3390, 1745, 1676, 1646, 1445, 1378, 1162 cm^{-1} ; ^1H and ^{13}C NMR (see Table 2); HRESIMS $[\text{M} + \text{H}]^+ m/z$ 494.2293 (calcd. for $\text{C}_{27}\text{H}_{32}\text{N}_3\text{O}_6$, 494.2286).

Versicamide G (7). White amorphous solid; $[\alpha]_{\text{D}}^{25} +36$ (c 0.1, CHCl_3); UV (MeOH) λ_{\max} (log ϵ) 264 (4.5), 287 (3.9), 296 (3.7), 325 (3.6); ECD (1.08×10^{-3} M, MeOH) λ_{\max} ($\Delta\epsilon$) 350 (+0.14), 319 (+4.09), 279sh (−1.63), 254 (−12.21), 223 (−3.43), 208 (−5.72) nm; IR (KBr) ν_{\max} 3370, 1680, 1594, 1373, 1261, 1115 cm^{-1} ; ^1H and ^{13}C NMR (see Table 2); HRESIMS $[\text{M} + \text{H}]^+ m/z$ 462.2024 (calcd. for $\text{C}_{26}\text{H}_{28}\text{N}_3\text{O}_5$, 462.2023).

Versicamide H (8). White amorphous solid; $[\alpha]_{\text{D}}^{25} +32$ (c 0.11, CHCl_3); UV (MeOH) λ_{\max} (log ϵ) 263 (4.5), 287 (3.9), 296 (3.7), 325 (3.6); ECD (1.09×10^{-3} M, MeOH) λ_{\max} ($\Delta\epsilon$) 357 (+0.18), 289 (−1.54), 250.4 (+3.33), 225.6 (−0.01), 208.6 (+2.19) nm; IR (KBr) ν_{\max} 3423, 1678, 1596, 1421, 1377, 1256, 1113 cm^{-1} ; ^1H and ^{13}C NMR (see Table 3); HRESIMS $[\text{M} + \text{H}]^+ m/z$ 458.2075 (calcd. for $\text{C}_{27}\text{H}_{28}\text{N}_3\text{O}_4$, 458.2074).

(−)-Enamide (9). White amorphous solid; $[\alpha]_{\text{D}}^{25} -112$ (c 0.1, MeOH); ECD (1.16×10^{-3} M, MeOH) λ_{\max} ($\Delta\epsilon$) 375.5 (−0.13), 332 (−0.39), 301.5 (−1.46), 259.5 (+0.82), 218.5 (−3.62) nm.

Notoamide E (10). $[\alpha]_{\text{D}}^{25} -30$ (c 0.1, MeOH) [lit. $[\alpha]_{\text{D}}^{20} -28$ (c 0.013, MeOH)].

Brevianamide F (11). $[\alpha]_{\text{D}}^{25} -61$ (c 0.1, MeOH) [lit. $[\alpha]_{\text{D}}^{25} -64$ (c 0.69, MeOH)].

Treatment of Versicamide D (4) with Trifluoroacetic Acid (TFA). Versicamide D (4, 2 mg) was dissolved in DMSO (2 mL), and then 1 μL of TFA was added at room temperature; the mixture was stirred for 10 days, affording a mixture of 4 and 7 (Supporting Information, Figure S9). The mixture was further purified with a C_{18} column eluted with 60% aqueous MeOH to yield 7 (1.5 mg), which was confirmed by HRESIMS $[\text{M} + \text{H}]^+ m/z$ 462.2026 and ^1H NMR (600 MHz, CDCl_3 adding TFA) spectrum (Supporting Information, Figures S10 and S11).

Methylation of Versicamide G (7). Versicamide G (7, 20 mg) was dissolved in dry tetrahydrofuran (10 mL) and then K_2CO_3 (20

mg) and MeI (40 mL) were added. The mixture was refluxed (70 °C) in an atmosphere of N_2 for 24 h, and it was filtered. The product of the reaction was vacuum-dried and then dissolved in MeOH. The reduction product was separated by HPLC (60:40 MeOH– H_2O) to yield compound 8 (12 mg).

Computation Section. Conformational searches were run employing the “systematic” procedure implemented in Spartan '14,²⁴ using MMFF (Merck molecular force field). All MMFF minima were reoptimized with DFT calculations at the B3LYP/6-31+g(d) or B3LYP/6-311+g(d,p) levels using the Gaussian09 program.²⁵ The geometry was optimized starting from various initial conformations, with vibrational frequency calculations confirming the presence of minima. Time-dependent DFT calculations were performed on lowest-energy conformation for each configuration using 30 excited states in vacuum. ECD spectra were generated using the program SpecDis²⁶ by applying a Gaussian band shape with 0.26–0.36 eV width from dipole–length rotational strengths. The dipole velocity forms yielded negligible differences.

X-ray Crystallographic Analysis of Compound 1. Single-crystal X-ray diffraction data were collected with Cu $K\alpha$ radiation at 293 K ($\lambda = 1.54184 \text{ \AA}$). The structure was solved by direct methods (SHELXS-97) and refined using full-matrix least-squares difference Fourier techniques. Carbon, oxygen, and nitrogen atoms were refined anisotropically. Hydrogen atoms were either refined freely with isotropic displacement parameters or were positioned with an idealized geometry and refined riding on their parent C atoms. Crystals suitable for X-ray diffraction were obtained by slow evaporation of a mixed solution in MeOH– CH_2Cl_2 – H_2O . Crystallographic data (excluding structure factors) for 1 have been deposited in the Cambridge Crystallographic Data Centre: CCDC reference number 973004. These data can be obtained, free of charge, from Cambridge Crystallographic Data Centre via http://www.ccdc.cam.ac.uk/data_request/cif.

Crystal Data for 1. Monoclinic, $\text{C}_{26}\text{H}_{27}\text{N}_3\text{O}_3$, space group C2 with $a = 42.4851(7) \text{ \AA}$, $b = 7.73880(10) \text{ \AA}$, $c = 14.2913(2) \text{ \AA}$, $\alpha = 90^\circ$, $\beta = 103.844^\circ$, $\gamma = 90^\circ$, $V = 4562.25(11) \text{ \AA}^3$, $Z = 8$, $T = 293(2) \text{ K}$, $D_c = 1.251 \text{ mg/mm}^3$, $\mu = 0.664 \text{ mm}^{-1}$, and $F(000) = 1824$. Crystal size: $0.36 \times 0.34 \times 0.3 \text{ mm}^3$. Independent reflections: 8246 with $R_{\text{int}} = 0.0202$. The final agreement factors are $R_1 = 0.0361$ and $wR_2 = 0.0957$ [$I > 2\sigma(I)$]. Flack parameter = 0.09(16).

Table 4. Inhibitory Rates of Compound 8 on Several PTKs (10 μ M) Determined by ELISA^a

compd	inhibitory rates (%)																		
	ROS1	IGF1R	c-Met	RON	TYRO3	FGFR1	KDR	c-Kit	Flt-1	Flt-3	RET	EGFR	ErbB4	c-Src	ABL	EPH-A2	PDGFR- α	PDGFR- β	
Compound 8 (10 μ M)	0	0	0	0	0	2.0	34.7	60.0	10.9	6.9	23.2	26.7	0.0	0.0	9.3	12.4	10.9	6.9	
Su11248 (1 μ M)								87.2	82.6	88.2	88.9	92.3	81.0				71.7	85.5	
BIBW2992 (1 μ M)																			
Dasatinib (1 μ M)																			
AEW541 (1 μ M)		87.7																	
PF2341066 (1 μ M)	100		100																
XL184 (1 μ M)				100	100														
AP24534 (1 μ M)						100	100												

^aThe inhibitory rates (%) were determined from the results of three separate tests ($n = 3$) and calculated using the equation $[1 - (A_{490}/A_{490 \text{ control}})] \times 100\%$.

■ ASSOCIATED CONTENT

📄 Supporting Information

Computational data of 3, 4, 7, 8, and 9; chemical conversion data from 4 to 7; HPLC analysis of the organic extracts of the strain; and HRESIMS and NMR spectra of compounds 1–8. This material is available free of charge via the Internet at <http://pubs.acs.org>.

■ AUTHOR INFORMATION

Corresponding Author

*Tel.: 0086-532-82031619. Fax: 0086-532-82033054. E-mail: dehaili@ouc.edu.cn.

Notes

The authors declare no competing financial interest.

■ ACKNOWLEDGMENTS

This work was financially supported by the National Natural Science Foundation of China (nos. 41176120 and 21372208), the National High Technology Research and Development Program of China (no. 2013AA092901), the NSFC-Shandong Joint Fund (no. U1406402), the Program for New Century Excellent Talents in University (no. NCET-12-0499), the Public Projects of State Oceanic Administration (no. 2010418022-3), and the Program for Changjiang Scholars and Innovative Research Team in University (no. IRT0944).

■ REFERENCES

- (1) Li, S. M. *Nat. Prod. Rep.* **2010**, *27*, 57–58.
- (2) Zhuravleva, O. I.; Afiyatullo, S. S.; Denisenko, V. A.; Ermakova, S. P.; Slinkina, N. N.; Dmitrenok, P. S.; Kim, N. Y. *Phytochemistry* **2012**, *80*, 123–131.
- (3) Baran, P. S.; Corey, E. J. *J. Am. Chem. Soc.* **2002**, *124*, 7904–7905.
- (4) Cai, X. S.; Luan, Y. P.; Kong, X. L.; Zhu, T. J.; Gu, Q. Q.; Li, D. H. *Org. Lett.* **2013**, *15*, 2168–2171.
- (5) Wang, W. L.; Zhu, T. J.; Tao, H. W.; Lu, Z. Y.; Fang, Y. C.; Gu, Q. Q.; Zhu, W. M. *Chem. Biodiversity* **2007**, *4*, 2913–2919.
- (6) Wang, W. L.; Lu, Z. Y.; Tao, H. W.; Zhu, T. J.; Fang, Y. C.; Gu, Q. Q.; Zhu, W. M. *J. Nat. Prod.* **2007**, *70*, 1558–1564.
- (7) Wang, F. Z.; Fang, Y. C.; Zhu, T. J.; Zhang, M.; Lin, A. Q.; Gu, Q. Q.; Zhu, W. M. *Tetrahedron* **2008**, *64*, 7986–7991.
- (8) Du, L.; Li, D. H.; Zhu, T. J.; Cai, X. S.; Wang, F. P.; Xiao, X.; Gu, Q. Q. *Tetrahedron* **2009**, *65*, 1033–1039.
- (9) Du, L.; Yang, X. Y.; Zhu, T. J.; Wang, F. P.; Xiao, X.; Park, H.; Gu, Q. Q. *Chem. Pharm. Bull.* **2009**, *57*, 873–876.
- (10) Du, L.; Feng, T.; Zhao, B. Y.; Li, D. H.; Cai, S. X.; Zhu, T. J.; Wang, F. P.; Xiao, X.; Gu, Q. Q. *J. Antibiot.* **2010**, *63*, 165–170.
- (11) Zhou, L. N.; Zhu, T. J.; Cai, S. X.; Gu, Q. Q.; Li, D. H. *Helv. Chim. Acta* **2010**, *93*, 1758–1763.
- (12) Gao, H. Q.; Liu, W. Z.; Zhu, T. J.; Mo, X. M.; Mándi, A.; Li, J.; Ai, J.; Gu, Q. Q.; Li, D. H. *Org. Biomol. Chem.* **2012**, *10*, 9501–9506.
- (13) Gao, H. Q.; Zhu, T. J.; Li, D. H.; Gu, Q. Q.; Liu, W. Z. *Arch. Pharm. Res.* **2013**, *36*, 952–956.
- (14) Cai, X. S.; Luan, Y. P.; Kong, X. L.; Zhu, T. J.; Gu, Q. Q.; Li, D. H. *Org. Lett.* **2013**, *15*, 2168–2171.
- (15) Greshock, T. J.; Grubbs, A. W.; Tsukamoto, S.; Williams, R. M. *Angew. Chem., Int. Ed.* **2007**, *46*, 2262–2265.
- (16) Kobayashi, M.; Aoki, S.; Gato, K.; Matsunami, K.; Kurosu, M.; Kitagawa, I. *Chem. Pharm. Bull.* **1994**, *42*, 2449–2451.
- (17) Tsukamoto, S.; Kato, H.; Greshock, T. J.; Hirota, H.; Ohta, T.; Williams, R. M. *J. Am. Chem. Soc.* **2009**, *131*, 3834–3835.
- (18) (a) Payne, A. D.; Skelton, B. W.; Wege, D.; White, A. H. *Eur. J. Org. Chem.* **2007**, *2007*, 1184–1195. (b) Friesen, R. W.; Vice, S. F.; Findlay, C. E.; Dmitrienko, G. I. *Tetrahedron Lett.* **1985**, *26*, 161–164.
- (19) Patrick, J. B.; Rosenblum, M.; Witkop, B. *Experientia* **1950**, *6*, 461.

- (20) Du, L.; Feng, T.; Zhao, B. Y.; Li, D. H.; Cai, S. X.; Zhu, T. J.; Wang, F. P.; Xiao, X.; Gu, Q. Q. *J. Antibiot.* **2010**, *63*, 165–170.
- (21) Mosmann, T. *J. Immunol. Methods.* **1983**, *65*, 55–63.
- (22) Skehan, P.; Storeng, R.; Scudiero, D.; Monks, A.; McMahon, J.; Vistica, D.; Warren, J. T.; Bokesch, H.; Kenney, S.; Boyd, M. R. *J. Natl. Cancer Inst.* **1990**, *82*, 1107–1112.
- (23) Lin, L. G.; Xie, H.; Li, H. L.; Tong, L. J.; Tang, C. P.; Ke, C. Q.; Liu, Q. F.; Lin, L. P.; Geng, M. Y.; Jiang, H. L.; Zhao, W. M.; Ding, J.; Ye, Y. *J. Med. Chem.* **2008**, *51*, 4419–4429.
- (24) *Spartan'14*; Wavefunction Inc.: Irvine, CA, 2013.
- (25) Frisch, M. J.; Trucks, G. W.; Schlegel, H. B.; Scuseria, G. E.; Robb, M. A.; Cheeseman, J. R.; Scalmani, G.; Barone, V.; Mennucci, B.; Petersson, G. A.; Nakatsuji, H.; Caricato, M.; Li, X.; Hratchian, H. P.; Izmaylov, A. F.; Bloino, J.; Zheng, G.; Sonnenberg, J. L.; Hada, M.; Ehara, M.; Toyota, K.; Fukuda, R.; Hasegawa, J.; Ishida, M.; Nakajima, T.; Honda, Y.; Kitao, O.; Nakai, H.; Vreven, T.; Montgomery, J. A., Jr.; Peralta, J. E.; Ogliaro, F.; Bearpark, M.; Heyd, J. J.; Brothers, E.; Kudin, K. N.; Staroverov, V. N.; Kobayashi, R.; Normand, J.; Raghavachari, K.; Rendell, A.; Burant, J. C.; Iyengar, S. S.; Tomasi, J.; Cossi, M.; Rega, N.; Millam, J. M.; Klene, M.; Knox, J. E.; Cross, J. B.; Bakken, V.; Adamo, C.; Jaramillo, J.; Gomperts, R.; Stratmann, R. E.; Yazyev, O.; Austin, A. J.; Cammi, R.; Pomelli, C.; Ochterski, J. W.; Martin, R. L.; Morokuma, K.; Zakrzewski, V. G.; Voth, G. A.; Salvador, P.; Dannenberg, J. J.; Dapprich, S.; Daniels, A. D.; Farkas, O.; Foresman, J. B.; Ortiz, J. V.; Cioslowski, J.; Fox, D. J. *Gaussian 09*, revision A.1; Gaussian, Inc.: Wallingford, CT, 2009.
- (26) Bruhn, T.; Hemberger, Y.; Schaumlöffel, A.; Bringmann, G. *SpecDis*, version 1.53; University of Wuerzburg: Wuerzburg, Germany, 2011.